The Company of Biologists

RESEARCH ARTICLE

IL-15Rα membrane anchorage in either *cis* or *trans* is required for stabilization of IL-15 and optimal signaling

Agnès Quéméner[1,2], Sébastien Morisseau[1,2,3,*], Rui P. Sousa[1,2,4,*], Kilian Trillet[1,2], Mike Maillasson[1,2,5], Isabelle Leray[1,2], Yannick Jacques[1,2], Johann Dion[5], Isabelle Barbieux[1,2], Marie Frutoso[1,2], Adèle D. Laurent[4], Jean-Yves Le Questel[4] and Erwan Mortier[1,2,5,‡]

ABSTRACT

Interleukin (IL)-15 plays an important role in the communication between immune cells. It delivers its signal through different modes involving three receptor chains: IL-15Rα, IL-2Rβ and IL-2Rγc. The combination of the different chains result in the formation of IL-15Rα/IL-2Rβ/γc trimeric or IL-2Rβ/γc dimeric receptors. In this study, we have investigated the role of the IL-15Rα chain in stabilizing the cytokine in the IL-2Rβ/γc dimeric receptor. By analyzing the key amino acid residues of IL-15 facing IL-2Rβ, we provide evidence of differential interfaces in the presence or in the absence of membrane-anchored IL-15Rα. Moreover, we found that the anchorage of IL-15Rα to the cell surface regardless its mode of presentation – i.e. *cis* or *trans* – is crucial for complete signaling. These observations show how the cells can finely modulate the intensity of cytokine signaling through the quality and the level of expression of the receptor chains.

KEY WORDS: Cytokine, Interleukin, Receptor, Interaction, T cells, NK cells, Contact

INTRODUCTION

Cytokines ensure communication between cells via their interaction with cell surface membrane-bound receptors, and play a crucial role in the regulation of the immune responses. Binding of cytokines to their receptors initiates the multimerization of the receptor chains and the intracellular signaling cascades leading to the cellular responses, such as cell differentiation, maturation, proliferation and survival. Membrane-bound cytokine receptors usually bind the cytokine by using highly specific molecular interactions to provide the tight regulation necessary for the control of physiological responses. However, cytokines are also characterized by their redundancy owing to shared receptors. For instance, cytokines belonging to the IL-2 family share a common gamma receptor chain, also called γc. The IL-2Rγc chain (hereafter referred to as γc) is essential for the response to IL-2, IL-4, IL-7, IL-9, IL-15 and IL-21, playing a pivotal role in immune cell homeostasis (Lin and Leonard, 2018). Indeed, its absence or mutations of it affect

signaling of the γc-dependent cytokines and cause X-linked severe combined immunodeficiency (X-SCID) disorders. Receptors for IL-4, IL-7, IL-9 and IL-21 are heterodimers formed by the γc chain and a specific α-chain, whereas the receptors for IL-2 and IL-15 are heterotrimers composed of the γc and IL-2Rβ chain common to both cytokines, and of a specific α-chain (Lin and Leonard, 2018).

Despite the nomenclature, IL-2Rβ (Tsudo et al., 1986; Sharon et al., 1986) presents structural homologies with α-chain receptors of the other cytokine members of the family (Wang et al., 2009). Interestingly, the α-receptor chains of IL-4, IL-7, IL-9 and IL-21 display a high affinity for their specific cytokines (10–100 pM), whereas IL-2Rβ binds both IL-2 and IL-15 with lesser affinity (~100 nM) (Lin and Leonard, 2018). The main difference between receptors for IL-2 and IL-15 is that IL-2 binds to the IL-2R α-chain with far less affinity (10 nM) than IL-15 binds to the IL-15R α-chain (50 pM) (Lin and Leonard, 2018). IL-2Rα and IL-15Rα also display original features, as they contain sushi domains responsible for the binding of the cytokines (Rickert et al., 2005; Chirifu et al., 2007). Interestingly, the short cytoplasmic tails of IL-2Rα and IL-15Rα in the presence of the IL-2Rβ/γc receptor do not seem to participate in the signal transduction (Anderson et al., 1995), suggesting that these chains behave more like accessory receptor chains, conferring the specificity to the respective cytokine, rather than receptors involved directly in cytokine signaling (Wang et al., 2009). However, signaling functions of the isolated IL-15/IL-15Rα complex, in the absence of IL-2Rβ, γc or both receptor chains, have been evidenced in epithelial cells, in melanoma and basal breast cancer cell lines (Stevens et al., 1997; Pereno et al., 2000; Marra et al., 2014).

The cytokine IL-2 is mainly produced by activated T cells, whereas IL-15 is mostly produced by antigen-presenting cells, such as dendritic cells, monocytes/macrophages but also epithelial cells and stromal cells. Both cytokines promote the proliferation, differentiation, and survival of mature T cells and the cytolytic activity of natural killer (NK) cells expressing the IL-2Rβ/γc dimeric receptor (Ma et al., 2006). The heterodimerization of IL-2Rβ and γc forming the IL-2Rβ/γc dimeric receptor in response to IL-2 or IL-15 leads to signaling through the activation of the JAK/Stat pathway. The JAK1 and JAK3 kinases associate with the intracellular domains of the IL-2Rβ and γc, respectively, and activate the Stat3 and Stat5 transcription factors by phosphorylation (Johnston et al., 1995). IL-2Rα can be upregulated in response to activation to sensitize T or NK cells to low concentrations of IL-2 (Leonard et al., 1984; Nikaido et al., 1984). Consequently, α-chains associate with IL-2Rβ and γc chains to form a high-affinity trimeric receptor. IL-2Rα is also constitutively expressed by regulatory T cells, forming a constitutive high-affinity trimeric receptor for IL-2 (Sakaguchi et al., 1995). IL-15Rα can be expressed on the surface of T or NK cells, forming an IL-15Rα/IL-2Rβ/γc trimeric receptor (Anderson

et al., 1995; Carson et al., 1997). However, IL-15Rα appears to be mainly expressed by antigen-presenting cells. It binds IL-15 with a high affinity, allowing a producing cell to present IL-15 in *trans* via IL-15Rα to a neighboring cell that expresses the IL-2Rβ/γc complex. This original mechanism of action is called IL-15 *trans*-presentation (Dubois et al., 2002; Burkett et al., 2004; Mortier et al., 2008). Thus, IL-15 can act both in *cis*, like IL-2, but also in *trans*. In addition, a soluble (s) form of IL-15Rα (sIL-15Rα) can act either as an antagonist of IL-15 action, competing with membrane-bound IL-15Rα for the binding of IL-15 (Mortier et al., 2004) or, as an agonist, forming an IL-15Rα/IL-15 complex activating the IL-2Rβ/γc dimeric receptor more efficiently than IL-15 alone (Giron-Michel et al., 2005; Mortier et al., 2006). Thus, numerous laboratories turned the latter observation into therapeutic applications to mimic *trans*-presentation of soluble IL-15Rα/IL-15 (sIL-15Rα/IL-15, also referred to as '*trans*-signaling' of IL-15Rα/IL-15) (Mortier et al., 2006; Rubinstein et al., 2006; Stoklasek et al., 2006). This raises the question whether IL-15 *trans*-signaling through sIL-15Rα/IL-15 complexes truly functions as IL-15 *trans*-presentation.

To address this question, we started our investigations from the observation that binding of IL-15 to the IL-2Rβ/γc dimeric receptor was mainly owing to the IL-2Rβ chain (100 nM), contributing to the majority of the binding properties of the heterodimeric receptor. Thus, in this study, we depict how IL-15 binds to the IL-2Rβ

chain – according to the absence or the presence of IL-15Rα – in the *cis* or in *trans* mode context. Taking advantage of directed mutagenesis together with molecular dynamics simulations, we further describe the involvement of the IL-15Rα chain in stabilizing IL-15 within the IL-2Rβ/γc dimeric receptor, making that cytokine unique in the IL-2 family cytokines.

RESULTS

The paradoxical action of soluble IL-15Rα regarding IL-15 signaling

To precisely evaluate the propensity of sIL-15Rα (hereafter referred to as sIL-15Rα) to exert its action in an agonistic or an antagonistic way (Fig. 1A), we took advantage of Kit225 cells, which express both IL-2Rβ/γc dimeric and IL-15Rα/IL-2Rβ/γc trimeric receptors. Furthermore, to evaluate the real impact of sIL-15Rα on the action of IL-15 in the IL-2Rβ/γc dimeric context, CRISPR-Cas9 technology was used to generate an original cell line (Kit225-15RαKO) bearing a deletion in the IL-15Rα gene. Genomic analysis revealed that the deletion resulted in a frameshift, leading to the expression of a truncated IL-15Rα lacking its sushi domain and thus unable to bind IL-15 (Fig. S1). As assessed by using flow cytometry, Kit225-15RαKO cells did not express detectable levels of IL-15Rα, whereas levels of IL-2Rβ and γc were comparable to those in Kit225 cells (Fig. 1B). Kit225 and Kit225-15RαKO cells
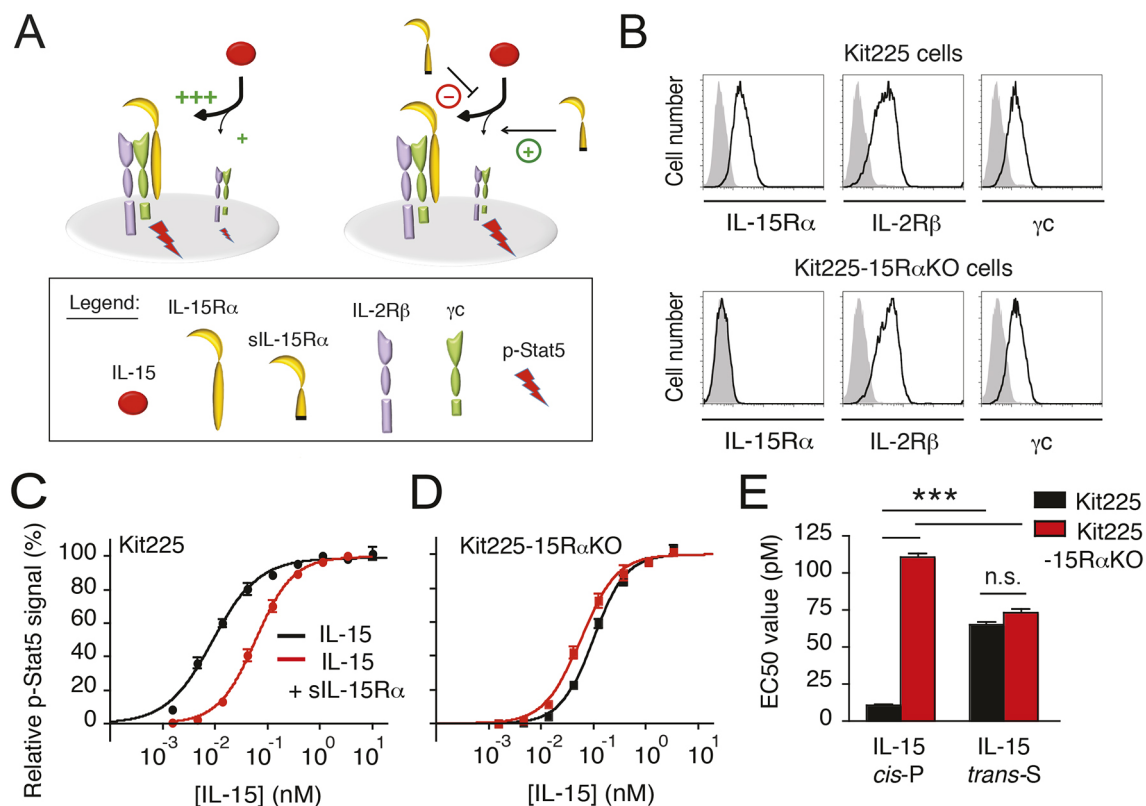

Fig. 1. The paradoxical action of soluble IL-15Rα on IL-15 signaling. (A) Diagram showing the different modes of action IL-15 has in *cis*. Left: IL-15 (red) can deliver its signal (red lightning) through the IL-2Rβ/γc dimeric receptor. The specific IL-15Rα (yellow) chain can be expressed together with IL-2Rβ (purple) and γc (green) on a same cell forming a high-affinity heterotrimeric receptor for IL-15 acting in *cis*: IL-15Rα/IL-2Rβ/γc *cis*-signaling. +++ and + indicate high and low p-Stat5 signal, respectively. Right: A soluble form of IL-15Rα (sIL-15Rα) can act either as an antagonist (–) of IL-15 action competing with membrane-bound IL-15Rα for the binding of IL-15, or as an agonist (+), forming an IL-15Rα/IL-15 complex activating IL-2Rβ/γc dimeric receptor more efficiently than IL-15 alone. (B) Flow cytometric analysis of IL-15Rα, IL-2Rβ and γc chains on Kit225 and Kit225-15RαKO cells. (C,D) Analysis of relative p-Stat5 levels in Kit225 cells (C) and Kit225-15RαKO cells (D) in response to increasing concentrations of IL-15 in the presence (red line) or absence (black line) of 100 nM sIL-15Rα. (E) Comparison of EC$_{50}$ values for p-Stat5 in Kit225 and Kit225-15RαKO cells in response to IL-15 in the presence or absence of sIL-15Rα. All data are representatives of at least three separate experiments. ***$P<0.001$; n.s., not significant.

Table 1. Analysis of p-Stat5 levels in Kit225 cells in response to increasing concentrations (1 pM–1 nM) of wt.IL-15 or its mutants in the presence or in absence of sIL-15Rα

| | p-Stat5 | | | |
| | | | sIL-15Rα (100 nM) | |
	EC_{50} (pM)	Relative activity (%)	EC_{50} (pM)	Relative activity (%)
wt.IL-15	11±1	100	65±8	100
IL-15$_{D8S}$	38±6	31±6	n.d.	n.d.
IL-15$_{S58K}$	24±2	37±3	194±22	24±1
IL-15$_{D61K}$	29±4	40±2	n.d.	n.d.
IL-15$_{E64K}$	19±6	75±21	687±281	9±1
IL-15$_{N65K}$	n.d.	n.d.	n.d.	n.d.
IL-15$_{I68K}$	195±62	6±1	n.d.	n.d.
IL-15$_{L69R}$	206±32	5±1	n.d.	n.d.
IL-15$_{N72K}$	5±0.5	117±4	66±6	54±6

EC_{50} and relative activity values (±s.e.m.) were calculated from the dose-response curves for Kit225 cells in response to wt.IL-15 (Fig. 1C) or its mutants (Fig. 4B).
Relative activity is the ratio of EC50 values for p-Stat5 responses to wt.IL-15 to those in response to mutants multiplied by 100.; n.d., not determined.

were exposed to increasing concentrations of IL-15 in the presence or absence of sIL-15Rα, and Stat5 phosphorylation was measured within the cells. We observed that the sensitivity of Kit225 cells to IL-15 was reduced 6-fold following the addition of sIL-15Rα; i.e. the half maximal effective concentration (EC_{50}) increased from 11 pM to 65 pM (Fig. 1C,E, and Table 1). As expected, for Kit225-15RαKO cells, the EC_{50} of phosphorylated Stat5 (p-Stat5) in response to increasing concentrations of IL-15 was 10-fold higher than for Kit225 cells (111 pM compared to 11 pM) (Fig. 1D,E), confirming that the presence of membrane-bound IL-15Rα chain improves the response to IL-15. Moreover, when IL-15 was associated to sIL-15Rα in Kit225-15RαKO cells, the EC_{50} of p-Stat5 was slightly decreased from 111 pM to 73 pM, indicating that sIL-15Rα could sensitize the cells expressing the IL-2Rβ/γc dimeric receptor to lower concentration of IL-15 (Fig. 1D,E, and Table 2). Interestingly, no difference was observed between the two cell lines when IL-15 had previously been associated with sIL-15Rα (Fig. 1E) as both EC50 values were measured to be ~70 pM. As expected, Stat5 phosphorylation induced by IL-2 stimulation of

Table 2. Analysis of p-Stat5 levels in Kit225-15RαKO cells in response to increasing concentrations (1 pM–1 nM) of wt.IL-15 or its mutants in the presence or in absence of sIL-15Rα

| | p-Stat5 in Kit225-15RαKO cells | | | |
| | | | sIL-15Rα (100 nM) | |
	EC_{50} (pM)	Relative activity (%)	EC_{50} (pM)	Relative activity (%)
wt.IL-15	111±9	100	73±10	100
IL-15$_{D8S}$	n.d.	n.d.	n.d.	n.d.
IL-15$_{S58K}$	599±23	18±1	326±35	21±1
IL-15$_{D61K}$	n.d.	n.d.	n.d.	n.d.
IL-15$_{E64K}$	6178±2121	2±1	893±370	8±1
IL-15$_{N65K}$	n.d.	n.d.	n.d.	n.d.
IL-15$_{I68K}$	n.d.	n.d.	n.d.	n.d.
IL-15$_{L69R}$	n.d.	n.d.	n.d.	n.d.
IL-15$_{N72K}$	168±8	39±3	67±7	125±76

EC_{50} and relative activity values (±s.e.m.) were calculated from the dose-response curves for Kit225-15RαKO cells in response to wt.IL-15 (Fig. 1D) or its mutants (Fig. 4A).
Relative activity is the ratio of EC50 values for p-Stat5 responses to wt.IL-15 to those in response to mutants, multiplied by 100.; n.d., not determined.

Kit225-15RαKO cells was not affected by the absence of IL-15Rα (Fig. S2). Thus, we were able to recapitulate both the agonistic and the antagonistic action of sIL-15Rα on IL-15 signaling within a same cell line context, allowing us to further investigate this differential effect.

Correlation between IL-15 residues that are involved in binding to IL-2Rβ and IL-15, and signal through the dimeric IL-2Rβ/γc receptor

As binding of IL-15 to the IL-2Rβ/γc dimeric receptor is mainly brought upon through the IL-2Rβ chain (Ring et al., 2012; Balasubramanian et al., 1995), we focused our interest on amino acid residues of IL-15 that are potentially involved in binding to this chain. Previous reports, including structural studies having used X-ray crystallography (Ring et al., 2012; Bernard et al., 2004; Pettit et al., 1997; Zhu et al., 2009), have identified helix C of IL-15 as a major player in this binding. Thus, we choose to analyze the exposed amino acid residues of IL-15 located on the helix C and directly face IL-2Rβ, i.e. D61, E64, N65, I68, L69 and N72 (Fig. S3A). We also included residue D8 on helix A, a residue that has already been described to play a significant role in IL-15 binding to IL-2Rβ (Pettit et al., 1997). To complete the identification of residues that interact with IL-2Rβ, molecular dynamics simulations were performed on the complex between IL-15 and its trimeric receptor. This led to the discovery that a further residue of IL-15, i.e. S58, is involved in binding to IL-2Rβ. As such, the molecular dynamics simulation brought S58 – located at the edge of the helix C of IL-15 – closer to S69 of the IL-2Rβ chain, thereby reducing and stabilizing the distance to their hydroxyl oxygen group from 7.1 Å to 3.7 Å to form an H-bond (Fig. 2A).

To evaluate the relative involvement of each of these IL-15 residues on binding to the IL-2Rβ chain, we performed directed mutagenesis. IL-15$_{S58K}$, IL-15$_{D61K}$, IL-15$_{E64K}$, IL-15$_{N65K}$, IL-15$_{I68K}$, IL-15$_{L69R}$ and IL-15$_{N72K}$ mutants were chosen on the basis of previous publications (Bernard et al., 2004; Pettit et al., 1997; Zhu et al., 2009) and a computational method (Spassov and Yann, 2013), allowing us to predict the free energy changes induced by mutation of exposed residues of IL-15 ($\Delta\Delta G_{mut}$) that are located on helix C to destabilize the interface (Fig. S3B). These mutants were produced in CHO cells, purified and their concentrations was measured by using calibration-free concentration analysis (CFCA). Their binding parameters to immobilized IL-2Rβ chain were then determined using surface plasmon resonance (SPR) analysis. We found that IL-15$_{D61K}$, IL-15$_{E64K}$, IL-15$_{N65K}$, IL-15$_{I68K}$ and IL-15$_{L69R}$ were unable to bind isolated IL-2Rβ, whereas IL-15$_{S58K}$ and IL-15$_{N72K}$ bound IL-2Rβ with K_d values comparable to that of wild-type IL-15 (wt.IL-15) (Fig. 2B and Table 3). Surprisingly, the IL-15$_{D8S}$ mutant was also capable to bind the IL-2Rβ chain albeit with an atypical kinetics curve, indicating that the D8 residue also has a role in binding to isolated IL-2Rβ. Moreover, by using a set of IL-15 and IL-15Rα antibodies, each of which specifically targets the IL-15/IL-15Rα, IL-15/IL-2Rβ or IL-15/γc interface, we showed that those sites of IL-15 that bind to IL-15Rα (M165 mAb) or γc (MAB247) were not affected by any of the mutations (Fig. S4). However, IL-15$_{D61K}$, IL-15$_{E64K}$, IL-15$_{N65K}$, IL-15$_{I68K}$ and IL-15$_{L69R}$ mutants were no longer able to bind the B-E29 anti-IL-15 mAb, one that targets the site IL-15 binds to IL-2Rβ and, especially, helix C (Mortier et al., 2004) – which is in contrast to IL-15$_{S58K}$, IL-15$_{N72K}$, IL-15$_{D8S}$ mutants and wt.IL-15. Taken together, these results confirm that helix C of IL-15 is the dominant factor of IL-15 for its binding to IL-2Rβ, and that amino acid residues D61, E64, N65, I68 and L69 are key contributors within helix C for this process.
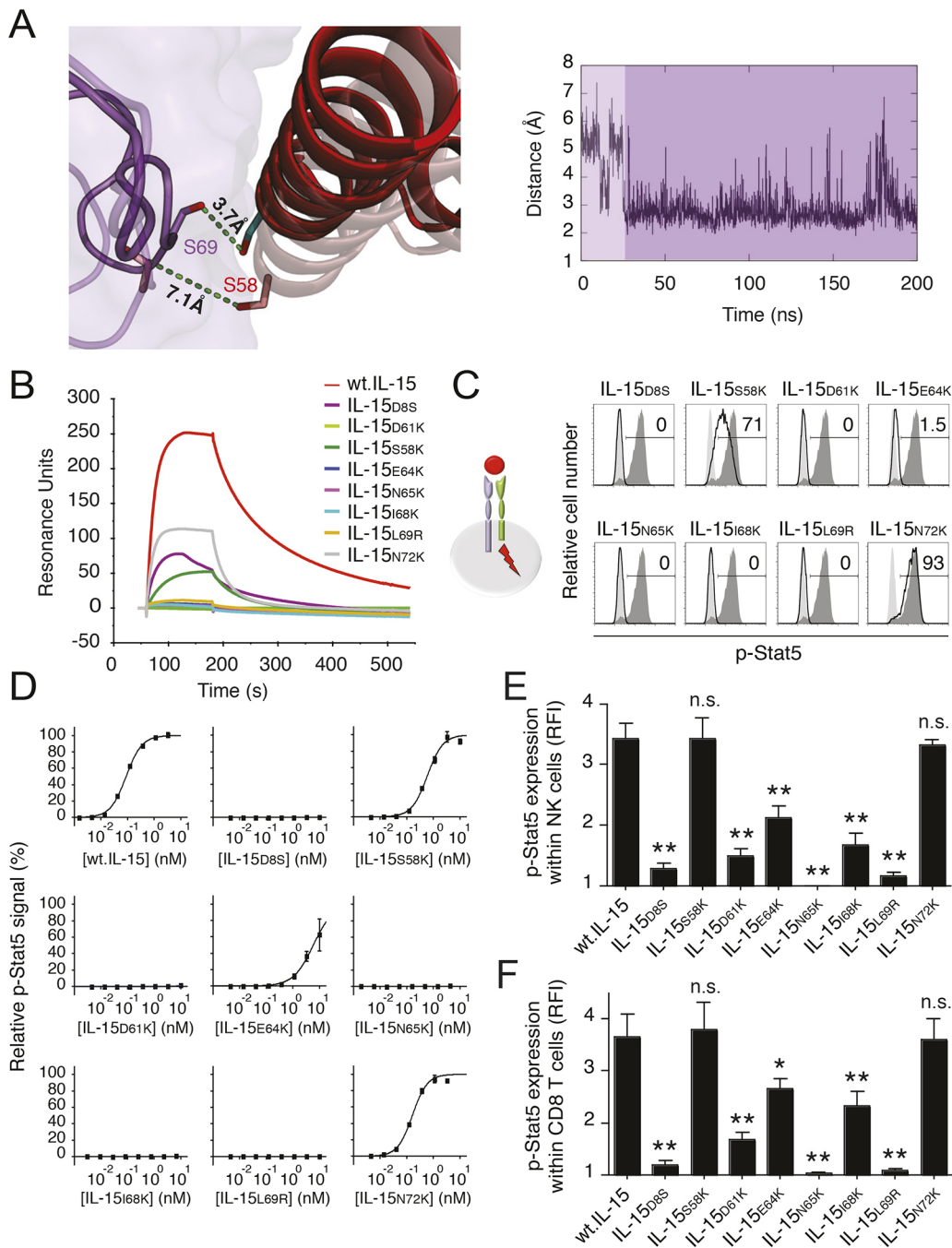
Fig. 2. Correlation between amino acid residues of IL-15 involved in binding to IL-2Rβ and in IL-15 signaling through the dimeric IL-2Rβ/γc receptor. (A) Left: Molecular dynamics simulation focused on S58 of IL-15 interacting with S69 of the IL-2Rβ chain. Right: Analysis of the distance (in Å) between the two residues during the 200 ns of molecular dynamics simulation. (B) SPR sensorgrams of wt.IL-15 or IL-15 mutant binding (both at 250 nM) to immobilized IL-2Rβ chain. (C) Flow cytometric analysis of p-Stat5 levels in Kit225-15RαKO cells in response to IL-15 mutants (at 100 pM) as indicated (black histograms). Numbers indicate the percentage of cells in the indicated gate corresponding to the black histogram. Dark grey filled histograms represent the p-Stat5 expression induced by wt.IL-15 and the light grey-filled histograms the isotype control. (D) Analysis of relative p-Stat5 levels in Kit225-15RαKO cells in response to increasing concentrations of wt.IL-15 or indicated IL-15 mutants, by AlphaScreen technology. (E,F) Primary NK or CD8T cells purified from human PBMCs. Analyses of p-Stat5 RFI levels in NK cells (E) and CD8T cells (F) in response to 1 nM of wt.IL-15 or indicated IL-15 mutants for 1 h. All data are representative of at least three separate experiments. *$P<0.05$, **$P<0.01$; n.s., not significant.

Next, using flow cytometry, the different IL-15 mutants were tested for their capacity to induce Stat5 phosphorylation within Kit225-15RαKO cells. wt.IL-15 and IL-15$_{N72K}$ induced full Stat5 phosphorylation at the two concentrations tested (100 pM and 1 nM; 93% for IL-15$_{N72K}$) (Fig. 2C, Fig. S5A), whereas that for IL-15$_{S58K}$ was reduced slightly at 100 pM (71%) (Fig. 2C)

and became comparable to that of wt.IL-15 at 1 nM. Interestingly, 60% of Kit225-15RαKO cells were positive for p-Stat5 when Kit225-15RαKO cells were submitted to 1 nM of IL-15$_{E64K}$ (Fig. S5A), whereas no signal was detected at 100 pM (Fig. 2C). Importantly, no p-Stat5 was detected when Kit225-15RαKO cells were exposed to IL-15$_{D8S}$, IL-15$_{D61K}$, IL-15$_{N65K}$,

Table 3. SPR analysis – parameters of wt.IL-15 and its mutants when bound to the immobilized IL-2Rβ chain

	K_d (nM)	R_{max} (RU)	Chi^2 (RU^2)
wt.IL-15	**37**	**267**	**1.02**
IL-15$_{D8S}$	414	148	37.9
IL-15$_{S58K}$	115	166	1.28
IL-15$_{D61K}$	n.d.	n.d.	n.d.
IL-15$_{E64K}$	n.d.	n.d.	n.d.
IL-15$_{N65K}$	n.d.	n.d.	n.d.
IL-15$_{I68K}$	n.d.	n.d.	n.d.
IL-15$_{L69R}$	n.d.	n.d.	n.d.
IL-15$_{N72K}$	64	166	1.98

R_{max}, is determined by the relative molecular weight ratio between ligand and analyte, and the amount of immobilized ligand (RU is an arbitrary unit that reflects the amount of complexes formed); Chi^2, gives a measure of the accuracy of the fitting (RU^2); n.d., not determined.

IL-15$_{I68K}$, and IL-15$_{L69R}$ at either concentration tested (Fig. 2C, Fig. S5A).

To further investigate the impact of the IL-15 point-mutations on its biological action through IL-2Rβ, we obtained p-Stat5 dose–response curves on Kit225-15RαKO cells by using AlphaScreen technology. The EC$_{50}$ of p-Stat5 in response to IL-15$_{S58K}$, IL-15$_{N72K}$ and IL-15$_{E64K}$ were measured to be ∼600 pM, 168 pM and ∼6 nM, respectively, whereas its EC$_{50}$ in response to wt.IL-15 was ∼111 pM (Fig. 2D, Table 2). Once again, no signal was detected at any concentration of IL-15$_{D8S}$, IL-15$_{D61K}$, IL-15$_{N65K}$, IL-15$_{I68K}$ or IL-15$_{L69R}$. Thus, in this IL-2Rβ/γc dimeric receptor context, the IL-15 residues involved in interaction with and signaling through the IL-2Rβ chain could be divided into two classes; those that are essential (D8, D61, N65, I68 and L69) and those that are only partially involved (E64>S58>N72).

We extended our investigations to human primary NK and CD8T cells, isolated from human peripheral blood mononuclear cells (PBMCs). Both cell types express the IL-2Rβ/γc dimeric receptor but only few or no IL-15Rα on their surface (Fig. S6). We observed that both NK and CD8T cells were able to phosphorylate Stat5 in response to wt.IL-15, IL-15$_{S58K}$ and IL-15$_{N72K}$ and, more weakly, in response to IL-15$_{E64K}$ and IL-15$_{I68K}$. Interestingly, low levels of p-Stat5 were detected when the cells were submitted to IL-15$_{D8S}$, IL-15$_{D61K}$ and IL-15$_{L69R}$. However, no p-Stat5 was detected in response to IL-15$_{N65K}$ in both cell types. Importantly, these results on naïve PBMCs are a fairly good confirmation of the ones obtained when using Kit225-15RαKO cells, except for IL-15$_{I68K}$ (Fig. 2E, F). Moreover, these biological observations are in accordance with the IL-2Rβ binding data (Fig. 2B, Table 3).

Involvement of membrane-bound IL-15Rα chain in IL-15 signaling

To evaluate the biological properties of the above IL-15 mutants on the IL-15Rα/IL-2Rβ/γc trimeric receptor, we took advantage of Kit225 cells that express both IL-2Rβ/γc dimeric and IL-15Rα/IL-2Rβ/γc trimeric receptors. Surprisingly, all mutants – except IL-15$_{N65K}$ – were able to induce Stat5 phosphorylation in these cells (Fig. 3A and Fig. S5B). However, the ratio between the mean fluorescence intensity (MFI) of IL-15Rα levels versus the MFI of the isotype control (hereafter referred to as RFI) of the amount of p-Stat5 within Kit225 cells in response to IL-15$_{L69R}$ and IL-15$_{I68K}$ was lower than that of wt.IL-15. These results suggest that membrane-bound IL-15Rα partially stabilizes IL-15 within the IL-2Rβ/γc receptor in a manner that requires the contact residue N65 of IL-15.

We extended our investigations to human primary NK and CD8T cells cultured in the presence of IL-2 to upregulate the expression of membrane-bound IL-15Rα (Fig. S6). For both cell types, we observed that p-Stat5 levels in response to wt.IL-15 were increased after culture in the presence of IL-2 (RFI=3–4 versus RFI=5–7; see Fig. 2E,F versus Fig. 3B, C) and that, interestingly, both cell types responded to every IL-15 mutants, except IL-15$_{N65K}$ (Fig. 3B,C).

To understand the crucial role of the residue N65 in IL-15 signaling both in the IL-15Rα/IL-2Rβ/γc trimeric receptor and the IL-2Rβ/γc dimeric receptor context, molecular dynamics simulations were performed using either wt.IL-15 or IL-15$_{N65K}$. The results revealed close contacts between wt.IL-15 and IL-2Rβ, although complementarity between IL-15$_{N65K}$ and IL-2Rβ was greatly affected (Fig. 3D,E, left panels). Moreover, we observed that N65 of wt.IL-15 within IL-2Rβ entered a 'hole' of the IL-2Rβ chain formed by the residues R42 and Q70 of IL-2Rβ chain making three hydrogen bonds (Fig. 3D, right panel and Fig. S7A). By contrast, K65 of the IL-15$_{N65K}$ mutant was interacting only with R41 of IL-2Rβ chain, generating only one hydrogen bond. In addition, the collateral consequences of the N65K mutation were dramatic, with a loss of most interaction between helix C and IL-2Rβ (Fig. 3E and Fig. S7B). To evaluate this potentially disparate effect, two different parameters were considered to compare the IL-15$_{N65K}$ mutant with the wild-type. For that, we established the total number of contacts between the residues at each side of interface between IL-15 and IL-2Rβ, and the free energy of helix C binding to IL-2Rβ, by using the molecular mechanics (MM) energies combined with the generalized Born and surface area continuum solvation (MM/GBSA) method. We observed that the total number of contacts was significantly and strongly decreased for the IL-15$_{N65K}$ mutant (8.4±2.8 contacts) as compared to wt.IL-15 (21.3±3.2 contacts; Fig. 3F). Accordingly, the variation in MM/GBSA energies followed the same tendency (Fig. 3G). Other IL-15 mutant interactions, i.e. IL-15$_{D8S}$ on helix A and IL-15$_{S58K}$, IL-15$_{D61K}$, IL-15$_{E64K}$, IL-15$_{I68K}$, IL-15$_{L69R}$ and IL-15$_{N72K}$ on helix C, were also analyzed using molecular dynamics simulations and displayed no significant differences, neither regarding MM/GBSA energies nor regarding the number of contacts when compared to wt.IL-15 (Fig. S7C,D), confirming the main role of N65 in IL-15 action. Together, these results indicate a difference between IL-15 residues involved in signaling through the IL-15 receptor (IL-15Rα/ IL-2Rβ/γc or IL-2Rβ/γc) in the presence or absence of the membrane-bound IL-15Rα chain. Moreover, we identified and confirmed the residue N65 of IL-15 as the unique hot spot for the binding to IL-2Rβ.

Membrane-bound IL-15Rα stabilizes IL-15 signaling better than does soluble IL-15Rα in *trans*

We have previously shown that a soluble form of IL-15Rα associated to IL-15 stabilizes the binding of IL-15 to IL-2Rβ (Meghnem et al., 2017). As expected, addition of sIL-15Rα to IL-15 slightly sensitized Kit225-15RαKO cells to IL-15, yielding lower p-Stat5 levels (Fig. 1D). Similarly, sIL-15Rα enhanced the phosphorylation of Stat5 within Kit225-15RαKO cells, induced by IL-15$_{S58K}$, IL-15$_{E64K}$ and IL-15$_{N72K}$ mutants, with EC$_{50}$ values showing a shift from 600 pM, 6.2 nM and 168 pM to 326 pM, 893 pM and 67 pM, respectively (Fig. 4A, Table 2). By contrast, sIL-15Rα was inefficient to sensitize cells to the mutants IL-15$_{D8S}$, IL-15$_{D61K}$, IL-15$_{N65K}$, IL-15$_{I68K}$, or IL-15$_{L69R}$. These results indicate that IL-15, whether associated or not to sIL-15Rα, recruits the same set of residues for the signaling through the IL-2Rβ/γc dimer.

To confirm that membrane-bound IL-15Rα was more potent than sIL-15Rα to induce an IL-15 signal, we introduced this soluble form on Kit225 cells. As expected from the results obtained with
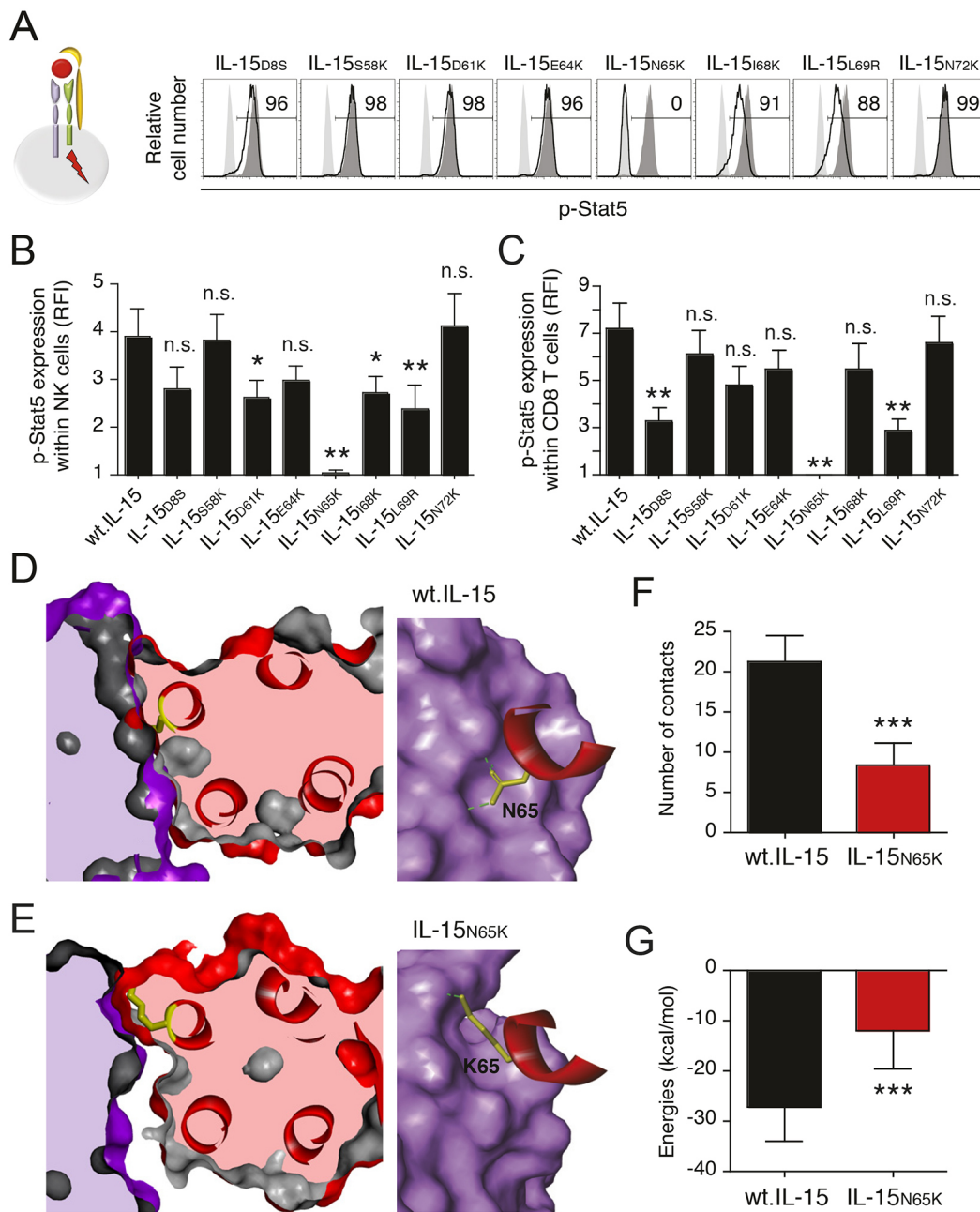
Fig. 3. Membrane-bound IL-15Rα stabilizes IL-15 signaling. (A) Diagram shows signaling of IL-15 through the IL-15Rα/IL-2Rβ/γc trimeric receptor (left). Flow cytometric analysis of p-Stat5 expression within Kit225 cells in response to indicated IL-15 mutants (black histogram) at 100 pM (right). Numbers indicate the relative cell number in percent cells within the indicated gate that corresponds to the black histogram. Dark grey filled histograms represent the p-Stat5 expression induced by wt.IL-15 and the light grey filled histograms the isotype control. (B,C) Primary NK or CD8T cells purified from human PBMCs and cultured in the presence of IL-2 for 5 days. Analyses of p-Stat5 levels in NK cells (B) and CD8T cells (C) in response to 1 nM of wt.IL-15 or 1 nM of different IL-15 mutants for 1 h. All data are representative of at least three separate experiments. (D,E) Left: wt.IL-15 (D, in red) or IL-15$_{N65K}$ (E, in red) interacting with IL-2Rβ (purple) after molecular dynamics simulations within an IL-15Rα/IL-2Rβ/γc complex. Right: Magnifications of IL-15 (N65, in yellow) and IL-15$_{N65K}$ (K65, in yellow), illustrating the interaction of each with the IL-2Rβ chain. (F) Analyses of the total number of contacts established within IL-15/IL-2Rβ (black) or IL-15$_{N65K}$/IL-2Rβ (red) interfaces during the molecular dynamics simulations (G) MM/GBSA energies. *$P<0.05$, **$P<0.01$, ***$P<0.001$; n.s., not significant.

wt.IL-15, sIL-15Rα switched IL-15$_{S58K}$, IL-15$_{E64K}$ and IL-15$_{N72K}$ action toward higher concentrations in the p-Stat5 assay, confirming that sIL-15Rα inhibits IL-15 signaling through the trimeric IL-15Rα/IL-2Rβ/γc receptor. EC50 values for p-Stat5 within Kit225 cells in response to wt.IL-15, IL-15$_{S58K}$, IL-15$_{E64K}$ or IL-15$_{N72K}$ were measured in the same range (11, 24, 19 or 5 pM, respectively) and increased between 6- and 36-fold in the presence of sIL-15Rα

(65, 194, 687 or 66 pM, respectively) (Fig. 4B and Table 1). Interestingly, these latter EC$_{50}$ values were equivalent to those obtained in Kit225-15RαKO cells with wt.IL-15, IL-15$_{S58K}$, IL-15$_{E64K}$ or IL-15$_{N72K}$ associated to sIL-15Rα (Tables 1 and 2). Moreover, the phosphorylation of Stat5 within Kit225 induced by IL-15$_{D8S}$, IL-15$_{D61K}$, IL-15$_{I68K}$ and IL-15$_{L69R}$ was completely inhibited by sIL-15Rα, indicating that signaling of these mutants is
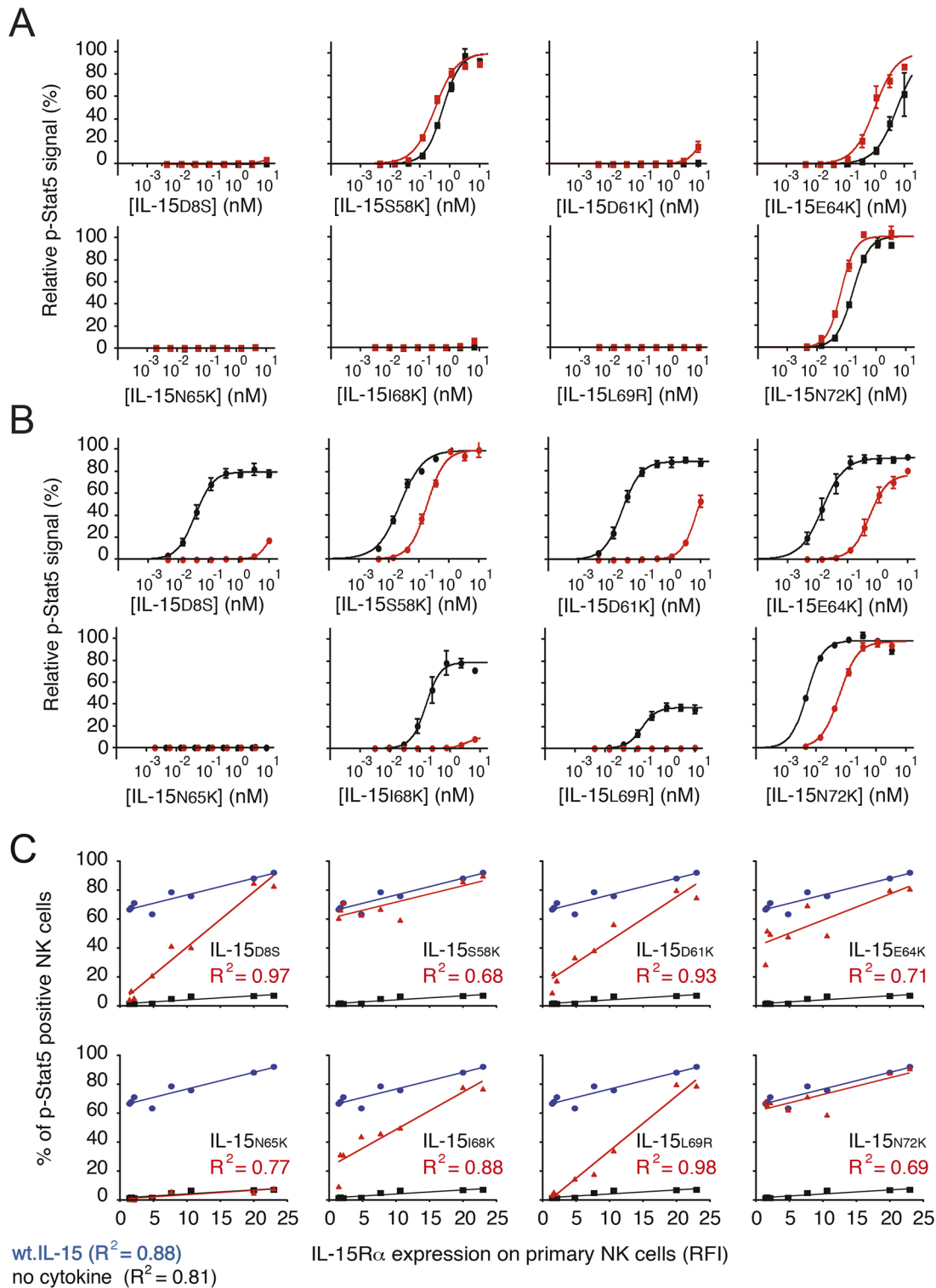
Fig. 4. Increasing levels of IL-15Rα gradually sensitize primary NK cells to IL-15. (A,B) Analysis of the relative p-Stat5 levels in Kit225-15RαKO (A) or Kit225 cells (B) in response to increasing concentrations of different IL-15 mutants in the presence (red line) or absence (black line) of 100 nM sIL-15Rα. All data are representative of at least three separate experiments. (C) Levels of p-Stat5 (pStat5)-positive NK cells in correlation to membrane levels of IL-15Rα in response to 1 nM of wt.IL-15 (blue), 1 nM of different IL-15 mutants (red) or no cytokine (black). The square of the coefficient correlation values, R^2, corresponding to the red linear regression curves of each IL-15 mutant are shown in each graph.

closely related to the presence of membrane-bound IL-15Rα (Fig. 4B). The EC_{50} values for p-Stat5 within Kit225 in response to IL-15$_{D8S}$, IL-15$_{D61K}$, IL-15$_{I68K}$ or IL-15$_{L69R}$ were estimated to be ~38, 29, 195 and 206 pM, respectively, but were not measurable

anymore in the presence of sIL-15Rα (Table 1). No p-Stat5 was detected in Kit225 and Kit225-15RαKO cells when using IL-15$_{N65K}$ (Fig. 4A,B), confirming the essential role for that residue also in this trimeric receptor configuration.

Increasing levels of IL-15Rα gradually sensitize primary NK cells to IL-15

Taking advantage of the heterogeneity of human blood samples regarding induction of IL-15Rα by IL-2, we found that the levels of IL-15Rα in NK cells measured by RFI varied between 1 and 24 (Fig. 4C). We observed that the levels of p-Stat5 within NK cells correlated to those of IL-15Rα, and increased from 70% to 100% in response to wt.IL-15 (R^2=0.88), IL-15$_{S58K}$ (R^2=0.68) and IL-15$_{N72K}$ (R^2=0.69). Interestingly, p-Stat5 levels in response to IL-15$_{D8S}$, IL-15$_{D61K}$ and IL-15$_{L69R}$ were not detectable in the absence of IL-15Rα but gradually increased in correlation with the IL-15Rα levels, to reach 100% (R^2=0.97, R^2=0.93, R^2=0.98, respectively). This confirms that these mutants fully depend on the presence of membrane-bound IL-15Rα. Intermediately, IL-15$_{E64K}$ and IL-15$_{I68K}$ were partially dependent on IL-15Rα, with a p-Stat5 levels of 30-40% to 100% (R^2=071, R^2=0.88, respectively) (Fig. 4C). Thus, these results confirm that membrane-bound IL-15Rα stabilizes IL-15 within the IL-2Rβ/γc dimeric receptor and that the levels of membrane IL-15Rα sensitizes NK cells to IL-15.

Comparison of the membrane-bound IL-15R α-chain in *cis* or *trans* regarding delivery of the IL-15 signal via the dimeric IL-2Rβ/γc receptor

We found evidence that membrane-bound IL-15Rα plays a major role in cells that coexpress IL-15Rα and the IL-2Rβ/γc receptor (IL-15Rα/IL-2Rβ/γc *cis*-signaling context, Fig. 3A, left panel). As IL-15 *trans*-presenting cells, we used HEK-293 cells stably transfected with IL-15Rα (IL-15Rα-HEK-293 cells) and expressing a high level of cell surface IL-15Rα that was loaded with increasing amounts of IL-15 (Tamzalit et al., 2014). We, thus, compared whether membrane-bound IL-15Rα in *trans* was as efficient as its *cis*-bound version in delivering the IL-15 signal through the IL-2Rβ/γc dimeric receptor. We analyzed Stat5 phosphorylation within Kit225 cells (IL-15Rα+) or Kit225-15RαKO (IL-15Rα−) in response to increasing amounts of IL-15 in *cis*- or *trans*-presented by IL-15Rα-HEK-293 cells. Surprisingly, we observed that IL-15 *trans*-presentation to Kit225-15RαKO cells was 10-fold more efficient (phosphorylation of Stat5) than its *cis*-signaling, whereas – on Kit225 cells – the two modes (*cis* and *trans*) had similar efficiencies (Fig. 5B,C). Importantly, the presence of IL-15Rα at the surface of Kit225 did not interfere with the *trans*-presentation of IL-15 in IL-15Rα-HEK-293 cells, as the EC$_{50}$ values of p-Stat5 in Kit225 or Kit225-15RαKO cells were not significantly different (Fig. 5C). Taken together, these results indicate that the cell membraneous IL-15Rα chain, regardless it is expressed by the responding cell expressing the IL-2Rβ/γc receptor or by a neighboring cell, is crucial for the stabilization of IL-15 to achieve complete IL-15 signaling.

Then, to evaluate the relative importance of IL-15 residues involved in interactions with IL-2Rβ when IL-15 is presented in *trans*, responding Kit225 cells were first labeled with Violet Proliferation dye 450 (VPD-450) to distinguish between cells that do and those that do not present IL-15. Kit225 cells were then cultured together IL-15Rα-HEK-293 cells to which IL-15 had been added (Tamzalit et al., 2014). Each IL-15 mutant was added at either 100 pM or 1 nM to IL-15Rα-expressing HEK-293 cells. After 1 h incubation, p-Stat5 levels within responding Kit225 cells was measured by flow cytometry. We found that IL-15$_{S58K}$, IL-15$_{E64K}$ and IL-15$_{N72K}$ at 1 nM or 100 pM, each were able to induce phosphorylation of Stat5 within responding Kit225 cells as efficiently as wt.IL-15 (Fig. 5D). Interestingly, p-Stat5 was also detected within Kit225 upon co-culturing with IL-15Rα-HEK-293

cells loaded with 1 nM of IL-15$_{D8S}$, IL-15$_{D61K}$ or IL-15$_{I68K}$, indicating that membrane-bound IL-15Rα expressed on IL-15-presenting cells was able to sensitize Kit225 such they responded to these mutants. However, IL-15$_{N65K}$ and IL-15$_{L69R}$, even when added at 1 nM, were unable to induce phosphorylation of Stat5 within responding Kit225 cells. Importantly, this signaling profile differs from those observed for IL-2Rβ/γc *cis*-signaling and soluble IL-15 *trans*-signaling.

Taken together, these results enabled us to refine and complete the molecular definition of the interface-binding area of IL-15 to IL-2Rβ, and to highlight the residues important in the different IL-15 modes of action, and we concluded the following (see Fig. 5E). Similar residues of IL-15 are involved in the action of IL-15 in a soluble way in the presence (*trans*-signaling) or in the absence (IL-2Rβ/γc *cis*-signaling) of sIL-15Rα. These show significant differences in their engagement when IL-15 is presented in a trimeric receptor context by membrane-bound IL-15Rα. In such a trimeric receptor context, the IL-15 residues of the interface area are similarly engaged, regardless whether IL-15 is presented by membrane-bound IL-15Rα in *cis* or in *trans*. The mechanism of IL-15 *trans*-presentation is more related to IL-15Rα/IL-2Rβ/γc *cis*-signaling than to soluble IL-15 *trans*-signaling.

DISCUSSION

Our current studies reveal an important role of membrane-bound IL-15Rα in facilitating the binding of IL-15 to IL-2Rβ and signaling through the IL-2Rβ/γc dimeric receptor. Moreover, we found a different implication of IL-15 residues to deliver a signal through IL-2Rβ/γc regarding membrane-bound IL-15Rα engagement or not. Indeed, we provided evidence that, in the absence of membrane-bound IL-15Rα, the IL-15 residues involved in binding to IL-2Rβ are correlated to those implicated in the signaling through the IL-2Rβ/γc dimeric receptor, which was not the case in the presence of membrane-bound IL-15Rα.

Involvement of IL-15/β interface residues differs depending on the type of receptor

Binding of IL-15 to the IL-2Rβ/γc dimeric receptor was mainly brought upon by interaction to IL-2Rβ. In this study, we extended our analysis of the IL-15/IL-2Rβ interface. Indeed, we have previously shown that IL-15$_{E64K}$, IL-15$_{N65K}$ and IL-15$_{I68K}$ mutants lead to defects in inducing proliferation in TF-1β cells that express the three IL-15 receptor chains (Bernard et al., 2004). Depicting further the binding interface between IL-15 and IL-2Rβ, we confirmed that amino acid residue N65 of IL-15, located on the helix C, is crucial for IL-15 binding as well as for signaling of IL-15. Moreover, we found that N65 plays a central role for the signaling regardless the mode of action of IL-15. Thus, we defined N65 to be the 'hot spot' of IL-15 signaling. This residue is located centrally within the interface area facing IL-2Rβ and is directed towards a binding pocket in IL-2Rβ (Ring et al., 2012). Structural analysis revealed that the N65 homolog of IL-15 on IL-2 is N88 (Wang et al., 2005). This asparagine residue was substituted by arginine (R), which presents properties similar to those of lysine (K) (Shanafelt et al., 2000). Interestingly, in contrast to IL-15$_{N65K}$, mutant IL-2$_{N88R}$ was signaling selectively through the IL-2Rα/IL-2Rβ/γc trimeric receptor, suggesting a different requirement of this residue regarding the signaling of these cytokines. However, in our current study, we evidenced that the IL-15 residues that surround N65 displayed behavior similar to that of IL-2$_{N88R}$. Indeed, IL-15$_{D8S}$, IL-15$_{D61K}$, IL-15$_{I68K}$ and IL-15$_{L69R}$ were able to signal through the trimeric receptor, whereas they were unable to bind IL-2Rβ and
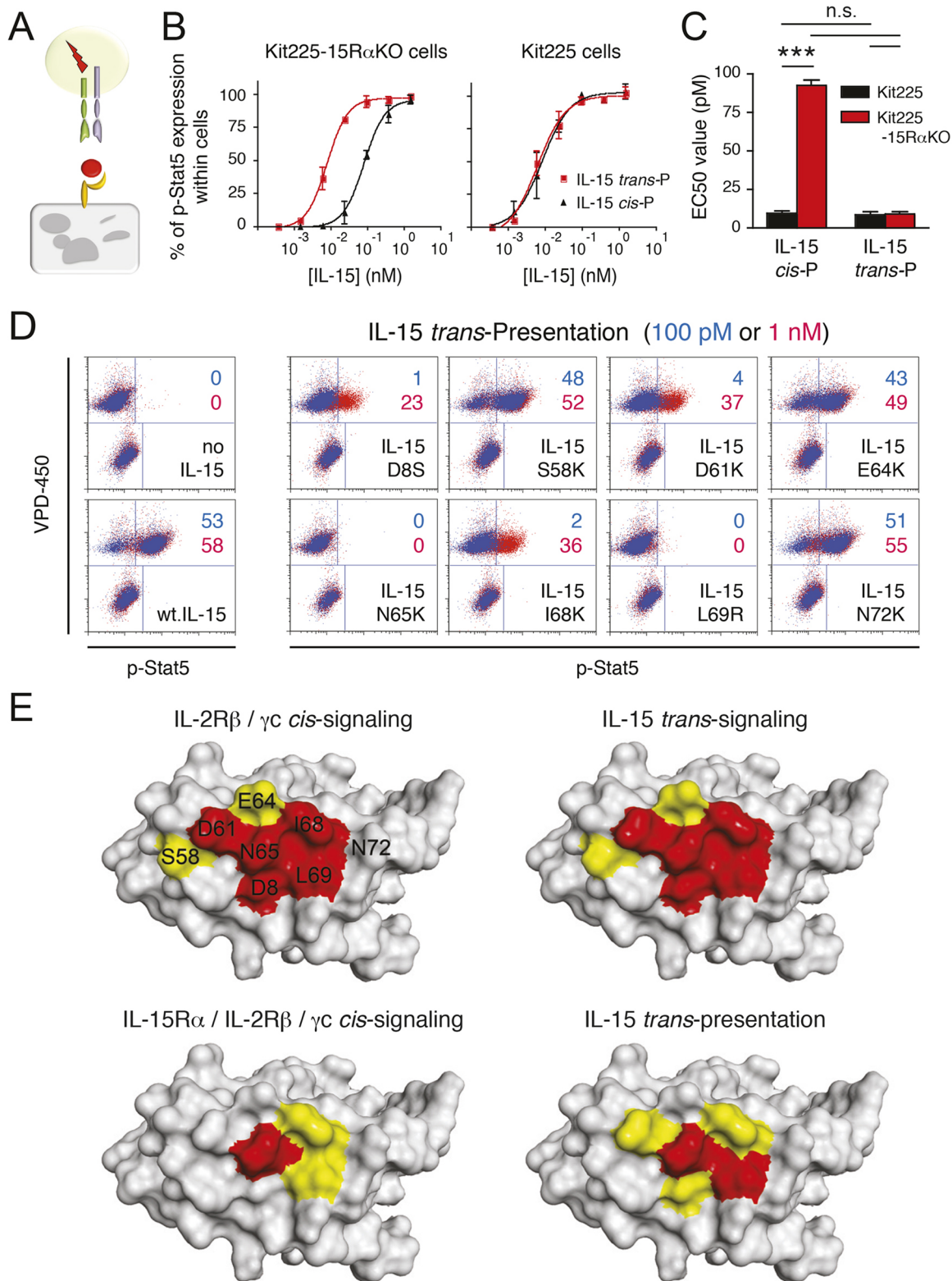
Fig. 5. Comparison of membrane-bound *cis* and *trans* IL-15Rα in delivering the IL-15 signal via the IL-2Rβ/γc receptor. (A) Diagram showing the IL-15 *trans*-presentation in which membrane-bound IL-15Rα expressed on one cell presents IL-15 in *trans* to neighboring cells that express the IL-2Rβ/γc dimeric receptor. (B) Flow cytometric analysis of p-Stat5 levels in Kit225-15RαKO cells (left) and Kit225 cells (right) in response to increasing concentrations of *cis*-presented wt.IL-15 (IL-15 *cis*-P, black) or *trans*-presented wt.IL-15 (IL-15 *trans*-P, red). (C) Comparative analysis of EC_{50} for p-Stat5 in Kit225-15RαKO cells (red bars) or Kit225 cells (black bars) in response to *cis*-presented wt.IL-15 (*cis*-P) or *trans*-presented wt.IL-15 (*trans*-P). ***$P<0.001$; n.s., not significant. (D) Flow cytometric analysis of p-Stat5 levels with in VPD-450-labeled Kit225 cells in response to 100 pM (blue) or 1 nM (red) wt.IL-15 or different IL-15 mutants loaded to IL-15Rα-HEK293 cells. All data are representatives of at least three separate experiments. (E) Comparison of binding areas of IL-15 within the indicated contexts, i.e. *cis/trans* signaling, *trans*-presentation. Residues crucial for IL-15 signaling are shown in red, those only partially involved are shown in yellow.

signal through the dimeric receptor. IL-15$_{E64K}$ was less selective for the trimeric receptor but still presented signaling – albeit impaired – through the IL-2Rβ/γc dimeric receptor. Accordingly, IL-2$_{D20K}$, the homolog of IL-15$_{D8S}$ located within helix A, was also selective for the IL-2Rα/IL-2Rβ/γc trimeric receptor and unable to induce proliferation of cells that expressed only the IL-2Rβ/γc dimer (Flemming et al., 1993; Arima et al., 1991). Thus, binding and signaling are not correlated when IL-15Rα or IL-2Rα chains formed a trimeric receptor together with IL-2Rβ/γc, suggesting that receptor α-chains are stabilizing binding of cytokine to the IL-2Rβ/γc dimeric receptor.

Role of IL-15Rα in IL-15 *trans*-signaling compared with IL-15 *trans*-presentation

It has been described that IL-6 can deliver a signal through *trans*-signaling, a mechanism by which IL-6 associated to soluble IL-6R can bind the IL-6 receptor subunit β (IL6ST, also known as gp130) on cells that do not express membrane-bound IL-6R and are unresponsive to IL-6 (Rose-John and Heinrich, 1994; Peters et al., 1996; Peters et al., 1998). In a similar way, we have previously shown that sIL-15Rα was increasing the binding affinity of IL-15 to IL-2Rβ, rendering the cells expressing IL-2Rβ and γc more sensitive to IL-15 (Mortier et al., 2006). This IL-15 *trans*-signaling has been compared to IL-15 *trans*-presentation, which requires membrane-bound IL-15Rα expressed on a neighboring cell (Dubois et al., 2002). However, associating sIL-15Rα to IL-15 only led to a slight increase of signaling via p-Stat5. Moreover, the residues involved in this signaling were comparable to those involved in signaling through IL-2Rβ/γc in the absence of IL-15Rα (IL-2Rβ/γc *cis*-signaling), but not to the common residue pattern found for IL-15Rα/IL-2Rβ/γc *cis*-signaling or *trans*-presentation. This suggests that the soluble form of IL-15Rα was not as efficient as membrane-bound IL-15Rα to stabilize IL-15 within the IL-2Rβ/γc dimeric receptor, despite increasing the affinity for IL-2Rβ. Thus, we suggest a dual role of IL-15Rα in IL-15 signaling, depending whether it is anchored to the membrane or not. Soluble IL-15Rα reinforces IL-15 binding to IL-2Rβ but this is not sufficient for complete signaling. Membrane-bound IL-15Rα, despite showing binding affinity to IL-15 that is identical to that of its soluble form (Mortier et al., 2004), better stabilizes IL-15 into the dimeric receptor. Our results, thus, further indicate that IL-15Rα anchorage to the cell membrane (in *cis* or in *trans*) plays an important role in stabilizing IL-15 within the IL-2Rβ/γc dimeric receptor. However, it cannot be excluded that our observations are restricted to our model. Indeed, several IL-15Rα isoforms from activated dendritic cells have been identified, among them, a soluble and secreted form named IC3-IL-15Rα (Müller et al., 2012). Interestingly, equimolar amounts of the soluble IC3-IL-15Rα/IL-15 complex were more efficient than the soluble wild-type IL-15Rα/IL-15 complex in stimulating the proliferation of PBMCs. It would, therefore, be of interest to identify the amino acid residues involved in the interface between IL-15 and this soluble IC3-IL-15Rα isoform, and compare them to those we identified in the present study.

Role of IL-15Rα in IL-15 *trans*-presentation compared with IL-15 *cis*-signaling

With respect to the provenance of membrane-bound IL-15Rα, we found that the efficacy of IL-15 signaling through the IL-15Rα/IL-2Rβ/γc trimeric receptor (IL-15Rα/IL-2Rβ/γc *cis*-signaling) and by *trans*-presentation were identical, with an estimated EC$_{50}$ of ~10 pM. Moreover, the interface areas facing the IL-2Rβ chain involved in *cis*- and *trans*-presentation were comparable, except

regarding residue L69. Indeed, no Stat5 phosphorylation was detected within responding cells when IL-15$_{L69R}$ was *trans*-presented. Interestingly L69 was the only residue used to distinguish between these two modes of action. This observation is in accordance with previous studies, showing that anti-IL-2Rβ A41 antibody inhibits IL-15 action through the IL-2Rβ/γc dimeric receptor (IL-2Rβ/γc *cis*-signaling), but is inefficient in blocking the IL-15Rα/IL-2Rβ/γc *cis*-signaling or the *trans*-presentation (Tamzalit et al., 2014; Lehours et al., 2000). We hypothesize that the absence of inhibitory effect of A41 can be explained by a conformational change initiated by membrane-bound IL-15Rα. Our present results further indicate that IL-15 *cis*- and *trans*-presentation signaling modes are comparable owing to IL-15Rα anchorage, regardless whether IL-15Rα is expressed in *cis* or in *trans*. This bi-directional property could be explained by the high affinity of IL-15 for isolated IL-15Rα. Regarding the IL-2 system, and despite few studies that suggest IL-2 can be *trans*-presented (Eicher and Waldmann, 1998; Wuest et al., 2011), this mode of action did not remain efficient because of the low affinity of isolated IL-2Rα. Indeed, high affinity is needed to retain the cytokine to the cell surface. To compensate this low affinity, several studies have suggested that IL-2Rα and IL-2Rβ are pre-complexed on the cell surface, resulting in a high-affinity dimeric receptor for IL-2. Consequently, the signaling of IL-2 can only be mono directional using the *cis* mode.

In summary, we identified certain amino acid residues of IL-15, located within the IL-15/IL-2Rβ interface, and their involvement in IL-15 signaling regarding its different mode of action. We, specifically, identified N65 within the IL-15/IL-2Rβ interface as a unique 'hot spot' of IL-15 signaling, which is common to all modes IL-15 signaling. Importantly, we provided evidence that anchorage of IL-15Rα is crucial for optimal *cis*- and *trans*-signaling, by highlighting the increased potency of IL-15 *trans*-presentation compared with that of IL-15 *trans*-signaling. These results give precious insights on how cytokines signal in a soluble or in a membrane-bound way.

MATERIALS and METHODS
Cell lines, recombinant proteins and antibodies

Kit225 and TF-1 cell lines were used and cultured as described previously (Bernard et al., 2004; Tamzalit et al., 2014). Healthy donor blood samples were collected from the French blood bank (Etablissement Français du Sang, Nantes). Peripheral blood mononuclear cells (PBMCs) were first isolated on a Ficoll (Eurobio Scientific) gradient, cleared for red blood cells with NH$_4$Cl solution (Stemcell Technologies) and stimulated or not with IL-2 (2 nM) for 5 days. Primary NK and T CD8$^+$ cells were sorted by using the NK cell isolation kit (Miltenyi Biotech) and human T CD8 MicroBeads (Miltenyi Biotech), respectively. All cell lines were maintained at 37°C, under a humidified 5% CO$_2$ atmosphere. Recombinant 6×His-tagged human IL-15 and its mutants, IL-15Rα sushi+ domain (residues 1–78) were produced by Evitria (Switzerland) and by using a HIS TRAP Excel column with an AKTA start system (Healthcare Life Sciences). Recombinant human IL-2 was purchased from Chiron (Suresnes, France). Recombinant soluble human IL-2Rβ protein (224-2B) was purchased from R&D Systems. Polyclonal goat anti-human IL-15Rα (AF247, used at a 1:100 dilution), polyclonal goat isotype control IgG (AB-108-C, used at a 1:1000 dilution) PE-conjugated donkey anti-goat IgG (F0107, used at a 1:400 dilution), and purified mouse IgG1 anti-human IL-15 (MAB247, used at a 1:1000 dilution) were all obtained from R&D Systems. Purified anti-human IL-15 (B-E29, used at a 1:1000 dilution) was purchased from Diaclone, anti-CD122 (TU27, used at a 1:1000 dilution) from Biolegend, anti-CD132 (TUGh4, used at a 1:1000 dilution) and mouse IgG1 (555-748, used at a dilution according to manufacturer's protocol) from BD Biosciences. Anti-human IL-15Rα M165 mAb (used at a 1:1000 dilution) was kindly provided

by GenMab (Copenhagen, Denmark). PE-conjugated goat F(ab′)2 anti-mouse IgG (H+L) (IM0855) was purchased from Beckman Coulter and used at a 1:200 dilution. For trans-presentation assay, Kit-225 cells were labeled with BD Horizon Violet Proliferation dye 450 (VPD-450; BD Biosciences).

Generation of Kit225-15RαKO

Guide RNA sequences targeting the exon 2 of IL-15Rα gene were designed and cloned into the T140-Cas9 plasmid by GenoCellEdit Platform (SFR Santé, Nantes). CRISPR knock-out Kit225 cells were generated by transfection with OFP plasmid followed by the selection of OFP+/IL-15Rα⁻ Kit225 cells by cell sorting (FACS Aria, BD Biosciences). Individual clones were generated by plating cells at low density and isolating individual colonies. IL-15Rα knock-out was confirmed by negative expression of IL-15Rα, and DNA sequencing. For sequencing, genomic loci were amplified by PCR using as forward primer (5′-TGACTGGCA-CTTAGGCG-3′) and as reverse primer (3′-TAGCCTCAGACCTCAGCA-CA-5′) and the DNA sequence of 11 clones was determined by the Genomic Platform (SFR Santé, Nantes). The sequencing results were aligned with NCBI reference sequences of IL-15Rα (NM 001256765.1).

Molecular interaction and CFCA

The SPR experiments were performed on a Biacore T200 biosensor (GE Healthcare). Recombinant IL2Rβ was covalently linked to CM5 sensor chips (GE Healthcare) using the amine coupling method in accordance to the manufacturer's instructions, and the binding of IL-15 or its mutants was monitored as described (Mortier et al., 2006). For calibration-free concentration analysis (CFCA), MAB247 anti-IL-15 antibody was immobilized to a CM5 sensor chip with the help of the amine coupling kit (GE Healthcare). Standard amine coupling procedures were followed and a flow rate of 10 µl/min was used for all injections. The coupling buffer was 10 mM sodium acetate (pH 5.0). Antibodies were immobilized in flow cell 2, with flow cell 1 being used as references. MAB247 antibody was injected over the flow cells 2 at 20 µg/ml in 10 mM acetate buffer (pH 5) for 10 min to reach a high immobilization level (∼10,000 RU). MAB247 antibody surfaces were regenerated between each CFCA cycle with 10 mM glycin (pH 2.0). All analyses were carried out in HEPES (pH 7.4) containing 0.15 M NaCl, 3.4 mM EDTA and 0.05% polysorbate. Protein samples were diluted from stock solutions to concentrations appropriate for CFCA (i.e. between 0.5 mM and 50 mM). CFCA was performed by adding samples at constant flow rate of 5 µl/min or 100 µl/min and 100 µl/min for 36 s over immobilized and reference surfaces. Buffer only was used as negative control. The Biacore T200 Evaluation 3.0 software (GE Healthcare) was used to run experiments and for data analysis.

p-Stat5 assays

Detection of p-Stat5 was carried out using either the AlphaLISA® SureFire® Ultra™ assay kit (PerkinElmer) or flow cytometry. For both assays, exponentially growing cells were starved overnight in the culture medium without cytokines. Cells were stimulated for 1 h at 37°C with increasing concentrations of IL-15 or its mutants pre-incubated or not with 100 nM IL-15Rα sushi+ domain.

For AlphaScreen assay, 2×10^5 stimulated cells were lysed and Stat5 phosphorylation was measured in the lysates, according to the manufacturer's instructions. The signal in the wells was then detected using an EnSpire Multimode Plate Reader (Perkin Elmer).

For flow cytometry p-Stat5 staining, 5×10^5 stimulated cells were fixed 10 min at 37°C using Fix Buffer I (BD Biosciences) and permeabilized in Perm Buffer III (BD Biosciences) 30 min at 4°C. Cells were then labeled with Phycoerythrin (PE)-conjugated mouse anti-human Stat5 (Y694) or PE-conjugated control isotype (BD Biosciences) for 1 h at room temperature. Cells were analyzed using a BD FACS Calibur, or BD FACS Canto 2 (BD Biosciences) and FlowJo software.

Molecular dynamics simulations

The initial coordinates for the molecular modeling study of IL-15 were extracted from the crystallographic data available on the Protein Data Bank for the IL-15/IL-15Rα/IL-2Rβ/γc (PDB ID: 4GS7) quaternary complexes

(Ring et al., 2012). The missing side-chain atoms, hydrogen atoms and disulfide bridges were added using the Prime tool in the Maestro program of the Schrödinger package (Schrödinger Release 201-1, Schrödinger, LLC, New York, NY, 2014). A missing loop on IL-15 (residues 25-31) was added by homology modelling considering an identical loop present on IL-2 (PDB ID 2B5I). The glycosylated residues in the original PDB files were restored to their non-glycosylated form. All H_2O molecules located in the crystallographic structure at 4 Å of the interface residues were kept.

In addition to the wt. IL-15, eight different mutants were used: IL-15$_{D8S}$ on helix A and IL-15$_{S58K}$, IL-15$_{D61K}$, IL-15$_{E64K}$, IL-15$_{N65K}$, IL-15$_{I68K}$, IL-15$_{L69R}$ and IL-15$_{N72K}$ on helix C using the Mutagenesis Wizard of PyMOL (Schrödinger, LLC; the PyMOL Molecular Graphics System, Version 1.8, 2015).

Molecular dynamics simulations were carried out using the NAMD program (Phillips et al., 2005) with the CHARMM36 force-field (Huang and MacKerell, 2013). To this end, the CHARMM-GUI tool was used for file preparation, which included the addition of explicit H_2O molecules (TIP3P model) (Jorgensen et al., 1983) in a cuboid box (dimensions: 12 Å) around the protein, and counter-ions in order to keep the system at a neutral charge. Initially, two energy minimizations of 10,000 steps were performed. In the first step, the H_2O molecules and counter-ions were minimized while the protein was kept fixed and, in the second, the whole system was minimized. Following these procedures, the system was heated to 300 K (26.85°C) for 200 ps (NVT ensemble), and the 200 ns production runs were performed (NPT ensemble). All these calculations were carried out with periodic boundary conditions, the Langevin thermostat being used to keep the temperature constant. The Particle-Mesh Ewald (PME) method was used to treat non-bonded interactions with a cut-off at 12 Å (Darden et al., 1993).

The total number of contacts between the analyzed residues on IL-15 and IL-2Rβ was calculated, for each frame of the trajectory in the interval for which the system was equilibrated (100–200 ns). This was performed using the 'nativecontacts' command of the 'cpptraj' trajectory analysis tool, present in the AmberTools18 collection of the Amber18 suite (Case et al., 2018). MM/GBSA energies were then calculated for each studied model, according to the following equation:

$$\Delta G_{bind} = G_{IL-15/IL-2Rb} - (G_{IL-15} + G_{IL-2Rb})$$

ΔG_{bind} corresponds to an average of the energy values computed for all snapshots between 100-200 ns.

Statistics

Statistical analyses were performed using one-way ANOVA tests (GraphPad Prism Software). Data are expressed as mean±s.e.m. A P value <0.05 was considered as significant (*P<0.05, **P<0.01, ***P<0.001). R2 is the squared value of the correlation coefficient for linear regressions.

the Nantes project of European Center of Transplantation and Immunotherapy Sciences (IHU-Cesti) through the ANR-10-IBHU-005 project, which received French government financial support managed by the Agence nationale de la recherche (ANR) and supported by Nantes Métropole and Pays de la Loire Région.

Supplementary information
Supplementary information available online at
http://jcs.biologists.org/lookup/doi/10.1242/jcs.236802.supplemental

References
Anderson, D. M., Kumaki, S., Ahdieh, M., Bertles, J., Tometsko, M., Loomis, A., Giri, J., Copeland, N. G., Gilbert, D. J., Jenkins, N. A. et al. (1995). Functional characterization of the human interleukin-15 receptor alpha chain and close linkage of IL15RA and IL2RA genes. *J. Biol. Chem.* **270**, 29862-29869. doi:10.1074/jbc.270.50.29862

Arima, N., Kamio, M., Okuma, M., Ju, G. and Uchiyama, T. (1991). The IL-2 receptor alpha-chain alters the binding of IL-2 to the beta-chain. *J. Immunol.* **147**, 3396-3401.

Balasubramanian, S., Chernov-Rogan, T., Davis, A. M., Whitehorn, E., Tate, E., Bell, M. P., Zurawski, G. and Barrett, R. W. (1995). Ligand binding kinetics of IL-2 and IL-15 to heteromers formed by extracellular domains of the three IL-2 receptor subunits. *Int. Immunol.* **7**, 1839-1849. doi:10.1093/intimm/7.11.1839

Bernard, J., Harb, C., Mortier, E., Quéméner, A., Meloen, R. H., Vermot-Desroches, C., Wijdeness, J., van Dijken, P., Grötzinger, J., Slootstra, J. W. et al. (2004). Identification of an interleukin-15α receptor-binding site on human interleukin-15. *J. Biol. Chem.* **279**, 24313-24322. doi:10.1074/jbc.M312458200

Burkett, P. R., Koka, R., Chien, M., Chai, S., Boone, D. L. and Ma, A. (2004). Coordinate expression and trans presentation of interleukin (IL)-15Rα and IL-15 supports natural killer cell and memory CD8+ T cell homeostasis. *J. Exp. Med.* **200**, 825-834. doi:10.1084/jem.20041389

Carson, W. E., Fehniger, T. A., Haldar, S., Eckhert, K., Lindemann, M. J., Lai, C. F., Croce, C. M., Baumann, H. and Caligiuri, M. A. (1997). A potential role for interleukin-15 in the regulation of human natural killer cell survival. *J. Clin. Invest.* **99**, 937-943. doi:10.1172/JCI119258

Case, D. A., Ben-Shalom, I. Y., Brozell, S. R., Cerutti, D. S., Cheatham, T. E., III, Cruzeiro, V. W. D., Darden, T. A., Duke, R. E., Ghoreishi, D., Gilson, M. K. et al. (2018). *AMBER 2018*. San Francisco: University of California.

Chirifu, M., Hayashi, C., Nakamura, T., Toma, S., Shuto, T., Kai, H., Yamagata, Y., Davis, S. J. and Ikemizu, S. (2007). Crystal structure of the IL-15-IL-15Rα complex, a cytokine-receptor unit presented in trans. *Nat. Immunol.* **8**, 1001-1007. doi:10.1038/ni1492

Darden, T., York, D. and Pedersen, L. (1993). Particle mesh Ewald: An N–log(N) method for Ewald sums in large systems. *J. Chem. Phys.* **98**, 10089-10092. doi:10.1063/1.464397

Dubois, S., Mariner, J., Waldmann, T. A. and Tagaya, Y. (2002). IL-15Rα recycles and presents IL-15 in trans to neighboring cells. *Immunity* **17**, 537-547. doi:10.1016/S1074-7613(02)00429-6

Eicher, D. M. and Waldmann, T. A. (1998). IL-2Rα on one cell can present IL-2 to IL-2R beta/gamma(c) on another cell to augment IL-2 signaling. *J. Immunol.* **161**, 5430-5437.

Flemming, C. L., Russell, S. J. and Collins, M. K. L. (1993). Mutation of Asp20 of human interleukin-2 reveals a dual role of the p55 α chain of the interleukin-2 receptor. *Eur. J. Immunol.* **23**, 917-921. doi:10.1002/eji.1830230423

Giron-Michel, J., Giuliani, M., Fogli, M., Brouty-Boyé, D., Ferrini, S., Baychelier, F., Eid, P., Lebousse-Kerdilès, C., Durali, D., Biassoni, R. et al. (2005). Membrane-bound and soluble IL-15/IL-15Rα complexes display differential signaling and functions on human hematopoietic progenitors. *Blood* **106**, 2302-2310. doi:10.1182/blood-2005-01-0064

Huang, J. and MacKerell, A. D. (2013). CHARMM36 all-atom additive protein force field: validation based on comparison to NMR data. *J. Comput. Chem.* **34**, 2135-2145. doi:10.1002/jcc.23354

Johnston, J. A., Bacon, C. M., Finbloom, D. S., Rees, R. C., Kaplan, D., Shibuya, K., Ortaldo, J. R., Gupta, S., Chen, Y. Q. and Giri, J. D. (1995). Tyrosine phosphorylation and activation of STAT5, STAT3, and Janus kinases by interleukins 2 and 15. *Proc. Natl. Acad. Sci. USA* **92**, 8705-8709. doi:10.1073/pnas.92.19.8705

Jorgensen, W. L., Chandrasekhar, J., Madura, J. D., Impey, R. W. and Klein, M. L. (1983). Comparison of simple potential functions for simulating liquid water. *J. Chem. Phys.* **79**, 926-935. doi:10.1063/1.445869

Lehours, P., Raher, S., Dubois, S., Guo, J., Godard, A. and Jacques, Y. (2000). Subunit structure of the high and low affinity human interleukin-15 receptors. *Eur. Cytokine Netw.* **11**, 207-215.

Leonard, W. J., Depper, J. M., Crabtree, G. R., Rudikoff, S., Pumphrey, J., Robb, R. J., Krönke, M., Svetlik, P. B., Peffer, N. J., Waldmann, T. A. et al. (1984). Molecular cloning and expression of cDNAs for the human interleukin-2 receptor. *Nature* **311**, 626-631. doi:10.1038/311626a0

Lin, J.-X. and Leonard, W. J. (2018). The common cytokine receptor γ chain family of cytokines. *Cold Spring Harb. Perspect. Biol.* **10**, a028449. doi:10.1101/cshperspect.a028449

Ma, A., Koka, R. and Burkett, P. (2006). Diverse functions of IL-2, IL-15, and IL-7 in lymphoid homeostasis. *Annu. Rev. Immunol.* **24**, 657-679. doi:10.1146/annurev.immunol.24.021605.090727

Marra, P., Mathew, S., Grigoriadis, A., Wu, Y., Kyle-Cezar, F., Watkins, J., Rashid, M., De Rinaldis, E., Hessey, S., Gazinska, P. et al. (2014). IL15RA drives antagonistic mechanisms of cancer development and immune control in lymphocyte-enriched triple-negative breast cancers. *Cancer Res.* **74**, 4908-4921. doi:10.1158/0008-5472.CAN-14-0637

Meghnem, D., Morisseau, S., Frutoso, M., Trillet, K., Maillasson, M., Barbieux, I., Khaddage, S., Leray, I., Hildinger, M., Quéméner, A. et al. (2017). Cutting edge: differential fine-tuning of IL-2- and IL-15-dependent functions by targeting their common IL-2/15Rβ/γc receptor. *J. Immunol.* **198**, 4563-4568. doi:10.4049/jimmunol.1700046

Mortier, E., Bernard, J., Plet, A. and Jacques, Y. (2004). Natural, proteolytic release of a soluble form of human IL-15 receptor α-chain that behaves as a specific, high affinity IL-15 antagonist. *J. Immunol.* **173**, 1681-1688. doi:10.4049/jimmunol.173.3.1681

Mortier, E., Quéméner, A., Vusio, P., Lorenzen, I., Boublik, Y., Grötzinger, J., Plet, A. and Jacques, Y. (2006). Soluble interleukin-15 receptor α (IL-15Rα)-sushi as a selective and potent agonist of IL-15 action through IL-15R beta/gamma. Hyperagonist IL-15xIL-15Rα fusion proteins. *J. Biol. Chem.* **281**, 1612-1619. doi:10.1074/jbc.M508624200

Mortier, E., Woo, T., Advincula, R., Gozalo, S. and Ma, A. (2008). IL-15Rα chaperones IL-15 to stable dendritic cell membrane complexes that activate NK cells via trans presentation. *J. Exp. Med.* **205**, 1213-1225. doi:10.1084/jem.20071913

Müller, J. R., Waldmann, T. A., Kruhlak, M. J. and Dubois, S. (2012). Paracrine and transpresentation functions of IL-15 are mediated by diverse splice versions of IL-15Rα in human monocytes and dendritic cells. *J. Biol. Chem.* **287**, 40328-40338. doi:10.1074/jbc.M112.378612

Nikaido, T., Shimizu, A., Ishida, N., Sabe, H., Teshigawara, K., Maeda, M., Uchiyama, T., Yodoi, J. and Honjo, T. (1984). Molecular cloning of cDNA encoding human interleukin-2 receptor. *Nature* **311**, 631-635. doi:10.1038/311631a0

Pereno, R., Giron-Michel, J., Gaggero, A., Cazes, E., Meazza, R., Monetti, M., Monaco, E., Mishal, Z., Jasmin, C., Indiveri, F. et al. (2000). IL-15/IL-15Rα intracellular trafficking in human melanoma cells and signal transduction through the IL-15Rα. *Oncogene* **19**, 5153-5162. doi:10.1038/sj.onc.1203873

Peters, M., Jacobs, S., Ehlers, M., Vollmer, P., Müllberg, J., Wolf, E., Brem, G., Meyer zum Büschenfelde, K. H. and Rose-John, S. (1996). The function of the soluble interleukin 6 (IL-6) receptor in vivo: sensitization of human soluble IL-6 receptor transgenic mice towards IL-6 and prolongation of the plasma half-life of IL-6. *J. Exp. Med.* **183**, 1399-1406. doi:10.1084/jem.183.4.1399

Peters, M., Blinn, G., Solem, F., Fischer, M., Meyer zum Büschenfelde, K. H. and Rose-John, S. (1998). In vivo and in vitro activities of the gp130-stimulating designer cytokine Hyper-IL-6. *J. Immunol.* **161**, 3575-3581.

Pettit, D. K., Bonnert, T. P., Eisenman, J., Srinivasan, S., Paxton, R., Beers, C., Lynch, D., Miller, B., Yost, J., Grabstein, K. H. et al. (1997). Structure-function studies of interleukin 15 using site-specific mutagenesis, polyethylene glycol conjugation, and homology modeling. *J. Biol. Chem.* **272**, 2312-2318. doi:10.1074/jbc.272.4.2312

Phillips, J. C., Braun, R., Wang, W., Gumbart, J., Tajkhorshid, E., Villa, E., Chipot, C., Skeel, R. D., Kalé, L. and Schulten, K. (2005). Scalable molecular dynamics with NAMD. *J. Comput. Chem.* **26**, 1781-1802. doi:10.1002/jcc.20289

Rickert, M., Wang, X., Boulanger, M. J., Goriatcheva, N. and Garcia, K. C. (2005). The structure of interleukin-2 complexed with its alpha receptor. *Science* **308**, 1477-1480. doi:10.1126/science.1109745

Ring, A. M., Lin, J.-X., Feng, D., Mitra, S., Rickert, M., Bowman, G. R., Pande, V. S., Li, P., Moraga, I., Spolski, R. et al. (2012). Mechanistic and structural insight into the functional dichotomy between IL-2 and IL-15. *Nat. Immunol.* **13**, 1187-1195. doi:10.1038/ni.2449

Rose-John, S. and Heinrich, P. C. (1994). Soluble receptors for cytokines and growth factors: generation and biological function. *Biochem. J.* **300**, 281-290. doi:10.1042/bj3000281

Rubinstein, M. P., Kovar, M., Purton, J. F., Cho, J.-H., Boyman, O., Surh, C. D. and Sprent, J. (2006). Converting IL-15 to a superagonist by binding to soluble IL-15Rα. *Proc. Natl. Acad. Sci. USA* **103**, 9166-9171. doi:10.1073/pnas.0600240103

Sakaguchi, S., Sakaguchi, N., Asano, M., Itoh, M. and Toda, M. (1995). Immunologic self-tolerance maintained by activated T cells expressing IL-2 receptor α-chains (CD25). Breakdown of a single mechanism of selftolerance causes various autoimmune diseases. *J. Immunol.* **155**, 1151-1164.

Shanafelt, A. B., Lin, Y., Shanafelt, M.-C., Forte, C. P., Dubois-Stringfellow, N., Carter, C., Gibbons, J. A., Cheng, S.-L., Delaria, K. A., Fleischer, R. et al. (2000). A T-cell-selective interleukin 2 mutein exhibits potent antitumor

activity and is well tolerated in vivo. *Nat. Biotechnol.* **18**, 1197-1202. doi:10.1038/81199

Sharon, M., Klausner, R. D., Cullen, B. R., Chizzonite, R. and Leonard, W. J. (1986). Novel interleukin-2 receptor subunit detected by cross-linking under high-affinity conditions. *Science* **234**, 859-863. doi:10.1126/science.3095922

Spassov, V. Z. and Yan, L. (2013). pH-selective mutagenesis of protein-protein interfaces: in silico design of therapeutic antibodies with prolonged half-life. *Proteins: Structure, Function, and Bioinformatics* **81**, 704-714. doi:10.1002/prot.24230

Stevens, A. C., Matthews, J., Andres, P., Baffis, V., Zheng, X. X., Chae, D. W., Smith, J., Strom, T. B. and Maslinski, W. (1997). Interleukin-15 signals T84 colonic epithelial cells in the absence of the interleukin-2 receptor beta-chain. *Am. J. Physiol.* **272**, G1201-G1208. doi:10.1152/ajpgi.1997.272.5.g1201

Stoklasek, T. A., Schluns, K. S. and Lefrançois, L. (2006). Combined IL-15/IL-15Rα immunotherapy maximizes IL-15 activity in vivo. *J. Immunol.* **177**, 6072-6080. doi:10.4049/jimmunol.177.9.6072

Tamzalit, F., Barbieux, I., Plet, A., Heim, J., Nedellec, S., Morisseau, S., Jacques, Y. and Mortier, E. (2014). IL-15.IL-15Rα complex shedding following trans-presentation is essential for the survival of IL-15 responding NK and T cells. *Proc. Natl. Acad. Sci. USA* **111**, 8565-8570. doi:10.1073/pnas.1405514111

Tsudo, M., Kozak, R. W., Goldman, C. K. and Waldmann, T. A. (1986). Demonstration of a non-Tac peptide that binds interleukin 2: A potential participant in a multichain interleukin 2 receptor complex. *Proc. Natl. Acad. Sci. USA* **83**, 9694-9698. doi:10.1073/pnas.83.24.9694

Wang, X., Rickert, M. and Garcia, K. C. (2005). Structure of the quaternary complex of interleukin-2 with its α, β, and γ_c receptors. *Science* **310**, 1159-1163. doi:10.1126/science.1117893

Wang, X., Lupardus, P., Laporte, S. L. and Garcia, K. C. (2009). Structural biology of shared cytokine receptors. *Annu. Rev. Immunol.* **27**, 29-60. doi:10.1146/annurev.immunol.24.021605.090616

Wuest, S. C., Edwan, J. H., Martin, J. F., Han, S., Perry, J. S. A., Cartagena, C. M., Matsuura, E., Maric, D., Waldmann, T. A. and Bielekova, B. (2011). A role for interleukin-2 trans-presentation in dendritic cell-mediated T cell activation in humans, as revealed by daclizumab therapy. *Nat. Med.* **17**, 604-609. doi:10.1038/nm.2365

Zhu, X., Marcus, W. D., Xu, W., Lee, H.-I., Han, K., Egan, J. O., Yovandich, J. L., Rhode, P. R. and Wong, H. C. (2009). Novel human interleukin-15 agonists. *J. Immunol.* **183**, 3598-3607. doi:10.4049/jimmunol.0901244